

PREDICTION OF FRETTING FATIGUE STRENGTH: PROPOSITION OF A FINITE ELEMENT BASED APPROACH

Alessandro Tavares da Silva Bernardo

Campus Universitário Darcy Ribeiro

Universidade de Brasília – UnB

Prédio da Faculdade Tecnologia – Bloco C

Departamento de Engenharia Mecânica – ENM

Asa Norte, Brasília-D.F.

C.E.P.: 70910-900

alebernardo@unb.br

José Alexander Araújo

alex07@unb.br

Edgar Nobuo Mamiya

mamiya@unb.br

Abstract. *The aim of this paper is the prediction of fatigue strength under fretting conditions by applying multiaxial criteria. A numerical approach using finite element modeling is proposed. The methodology is developed to incorporate the contact size effect observed in a number of experimental data available in the literature. The results obtained by the analysis agreed very well with these data.*

Keywords: fretting fatigue, finite element modeling, multiaxial fatigue criteria.

1. INTRODUÇÃO

Fretting fatigue is the cause of premature failure in a number of mechanical assemblies subjected to vibrations. Examples include riveted or bolted lap joints, spline couplings and fan blade/disc fixings (Shaffer, 1994). To gain a better understanding of this phenomenon, various experimental apparatus and methodologies have been developed (Kinyon, 2002) considering a number of different contact configurations (Shaffer, 1994; Harish, 1998; Wittkowsky, 1999).

In 1973, Bramhall (1973) first verified the existence of a critical contact size, dividing infinite and finite fretting fatigue regimes. These work revealed that for contact sizes smaller than the critical one lives were very long ($>10^8$ cycles), while for larger contacts lives were finite. Since then, new and better controlled experimental data have been produced by other researchers confirming the effect of the contact size on fretting life (Nowell 1988; Araújo, 1998). For instance, Nowell conducted experimental series using both flat “dog bone” specimens and cylindrical pads made of Al4%Cu alloy. The results provided by his work have been extensively considered to validate methodologies for prediction of fretting fatigue strength (Castro, 2003).

On the fretted surfaces, there may be a strong stress concentration that creates favorable conditions to crack nucleation. However, as the crack grows away from the surface, a high stress gradient will slow down such crack, so that it may eventually arrest (Araújo, 1999). Since not only the localized stress state, but also the stress gradient should be considered to model such problem,

the fretting fatigue life prediction of structural elements becomes a hard task (Hills, 1994). Moreover, previous works (Araújo, 2002; Fouvry, 2002; Castro, 2003) showed that the application of multiaxial fatigue criteria upon the fretting surface provide very conservative life estimates, although they may be useful to estimate both, the crack nucleation site (Fouvry, 2002) and the crack growth orientation (Swalla, 2003). In order to incorporate the effect of the stress gradient in the analysis many authors have considered a process volume approach (Araújo, 2002; Fouvry, 2002; Namjoshi, 2002; Naboulsi, 2003; Swalla, 2003), which consists in the application of the fatigue criteria upon the stress history approximated onto a volume rather than in a single point.

This paper is an attempt to make a finite element (FE) analysis of fretting fatigue by searching an appropriate mesh refinement level able to consider the stress gradient effect into the calculation of fatigue strength. The basic idea underlying such methodology is based on the fact that there is an intrinsic approximation of the stress state along a finite element due to the integral formulation of the method.

2. EXPERIMENTAL DATA

The FE analysis presented in this paper will be validated considering the work conducted by Nowell (1988). A schematic representation of the configuration tested is showed in Fig. 1a, where R is the radius of cylindrical fretting pad, P is the normal load, σ_B is the bulk stress and Q denotes the tangential load induced by the spring A . The contact loads P and Q and the bulk stress σ_B were applied as depicted in Fig. 1b, i.e., P is a static load and Q and σ_B are in phase sinusoidal functions of time. Five experimental series were conducted. In each one of this data series, the parameters p_0 (the peak pressure), Q_{max}/P and σ_{Bmax} , were kept constant, while the pad radius was varied from 12.5 to 150mm. Here the subscript *max* denotes the maximum value reached by Q and σ_B over time. These parameters for each series are presented in the Tab. 1. The importance of varying R keeping p_0 constant is that it is possible to produce a data series where all specimens are submitted to the same superficial stress state although they experience different stress decays. The tests carried out by Nowell revealed an effect of the pad radius (or contact size, a) on fretting life. It was observed that for small contact sizes fretting tests last infinitely while for large contacts specimens broke within a finite number of cycles. The range defined by the largest contact to show infinite life and the smallest contact to show finite life was termed (Bramhall, 1973) the *critical contact size* range, a_{crit} . Tab. 1 reports such range for each data series.

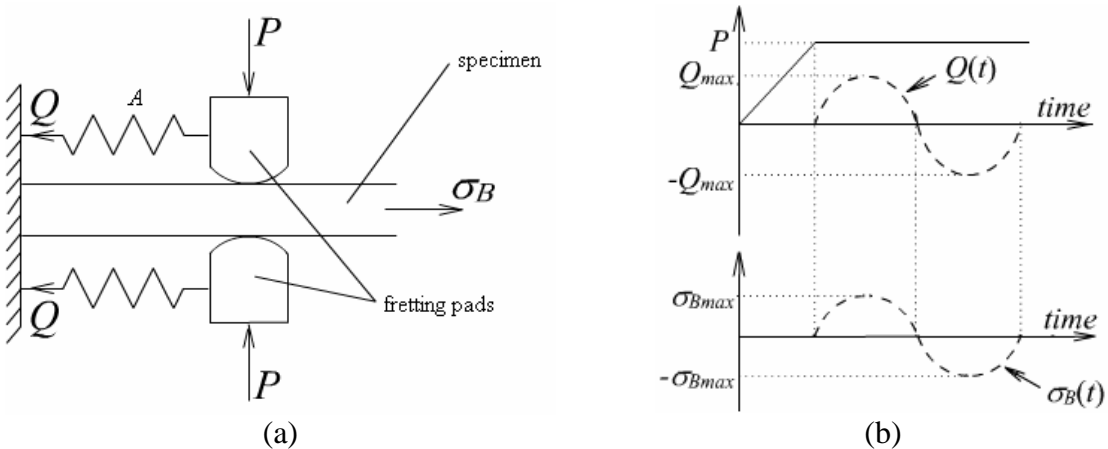


Figure 1. Nowell experimental configuration scheme.

Table 1. Experimental parameters and critical contact size.

Serie s	p_0 (MP a)	$\frac{Q_{\max}}{P}$	$\sigma_{B \max}$ (MPa)	a_{crit}
1	157	0.45	92.7	0.28–0.38
2	143	0.24	92.7	0.54–0.72
3	143	0.45	92.7	0.18–0.27
4	143	0.45	77.2	0.36–0.54
5	120	0.45	61.8	0.57–0.71

3. FE MODEL

To simulate the experiments, the FE code *ef++*, developed by the Mechanics of Materials Research Group of the University of Brasília, was considered. As a graphical interface this code uses the GiD platform (Ribó, 2000), which carries out both, pre – geometry creation, meshing and boundary conditions assignment – and post processing – stress, strain and displacement field visualization. A contact element was recently implemented (Bernardo, 2003) into the FE code, which allows the calculation of the stress field under fretting situations (Bernardo, 2003; Bernardo et. al., 2003). Moreover the Crossland (1956), Dang Van (1987) and Mamiya&Araújo (2002) multiaxial fatigue criteria have been implemented to the code (Dantas, 2002; Ferro, 2003) so that a direct fatigue strength analysis can be carried out. The program is able to apply these criteria on the nodal stress history.

In order to perform the FE analysis the model showed in Fig. 2 was adopted. Other fundamental parameters to the analysis are the material properties of the aluminum alloy used by Nowell (1988). They are: the Young's modulus ($E = 74$ GPa), the coefficient of friction ($f = 0.75$), the fatigue strength under alternate bending ($f_{-1} = 124$ MPa at 5×10^8 cycles). The fatigue strength under alternate torsion can be estimated for Al4%Cu as $t_{-1} = 72$ MPa at 5×10^8 cycles (Forrest, 1962; Bernardo, 2004).

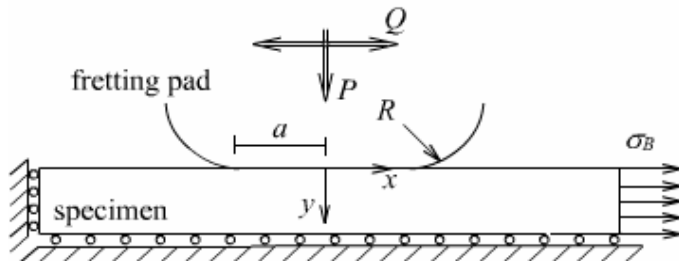


Figure 2. Scheme of the adopted model.

4. FE MESH

An example of a characteristic mesh generated for both fretting pad (150mm radius) and specimen is depicted in Fig. 3, where plane strain linear elastic triangular elements are used for the simulations. To simulate the contact problem bi-dimensional two-nodes interface elements were considered, as can be seen in Fig. 4. In the specimen domain a structured mesh region, near of the contact surface (Fig. 4) was defined. Within such region the mesh refinement level and the finite element size are characterized by three parameters, *viz*, the contact mesh width, l_c , and the element width and depth, l_e and h_e , respectively.

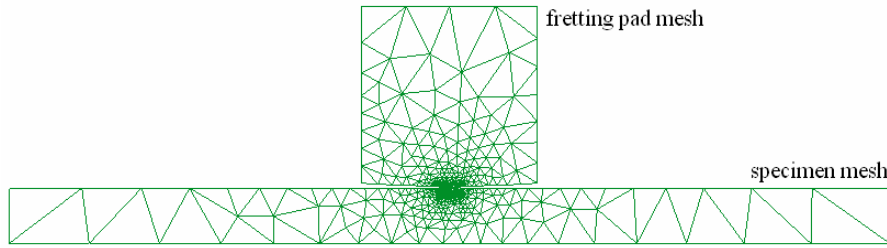


Figure 3. Mesh of both 150mm radii pad and specimen.

In a recent work conducted by one of the authors (Bernardo, 2004) it was shown that the numerically computed stress field for Nowell's contact configuration approximates well from the analytical solution for the adimensionalized parameters $l_c/a < 2.10$, $l_e/a < 0.0726$ and $h_e/a < 0.0146$. Furthermore, it should be reported that for l_e less than 20 μm and/or l_e/h_e ratio far from the unit, the numerical simulation becomes unstable. However, the aim of this work is not to generate a well refined mesh capable to capture the analytical stress field. As mentioned before there is a number of authors, including ourselves, who have tried to associate the contact size effect in fretting fatigue life with the presence of a stress gradient in the vicinity of the the contact region. In this paper it is claimed that such an effect can be incorporated to the calculation of the fatigue strength by choosing an appropriate mesh refinement level. The basic idea underlying such methodology is based on the fact that there is an intrinsic approximation of the stress state along a finite element due to the integral formulation of the method. Hence, the methodology proposed here is to vary the element size, which will provide different average stress states, until the numerical fatigue strength predictions match the experimental data.

The reader should notice that the usual FE procedure proposed by other authors (Naboulsi, 2003; Swalla, 2003) to incorporate the stress gradient in the fatigue strength analysis needs to determine the stress state, as accurately as possible, in a sufficiently large number of points (elements) within the process volume and then calculate the average volume stress. The approach developed in this work considers the finite element itself as the process volume. Thus the computational cost of the analysis is substantially reduced. Furthermore, it will be assessed in this paper whether the element size may be associated with material parameters such as the grain size. In order to do so, all fretting tests were simulated considering two sets of structured meshes having the same l_c but with two different l_e . For each set of structured mesh the element depth h_e assumed four different values, hence a total of eight different meshes were generated to assess the data.

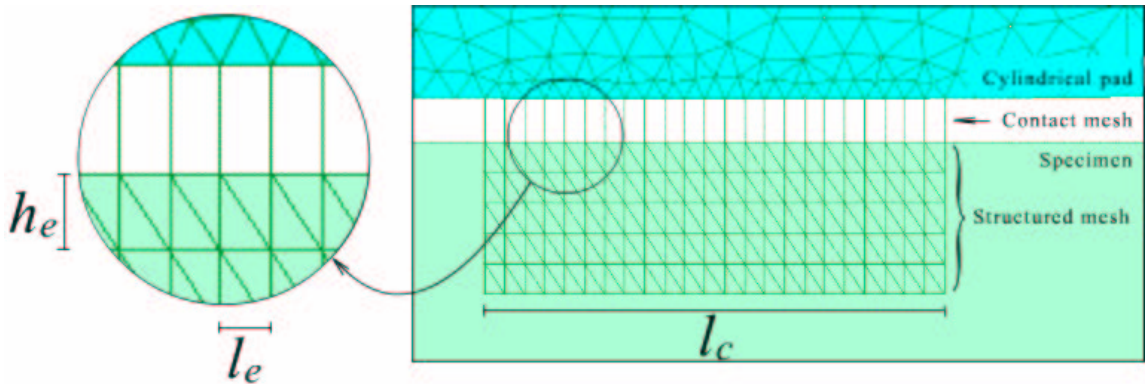


Figure 4. Mesh parameters.

5. RESULTS

Numerical simulations of fatigue strength have been conducted by considering the Crossland, Dang Van and Mamiya&Araújo, multiaxial models. Space only precludes us to present here a detailed description of these criteria, which have been well documented and discussed in the literature (Crossland, 1956; Dang Van, 1987; Papadopoulos, 1997; Mamiya&Araújo, 2002). The results of the numerical analysis are then compared with Nowell's experimental data. Following these results are presented and evaluated, but before an error index is defined. This parameter, which is obtained for each multiaxial fatigue criteria studied, is used to quantify the fatigue strength of a component.

5.1 Error Index Definition

A generic multiaxial fatigue criterion based on the stress invariant approach can be expressed by the inequality:

$$g_1(\tau) + \kappa g_2(\sigma) \leq \lambda, \quad (1)$$

where κ and λ are material constants, $g_1(\tau)$ is a function of the deviatoric stress history and $g_2(\sigma)$ denotes a function of the normal stress history. In this setting, an error index to compute the fatigue strength can be defined as:

$$I = \frac{g_1(\tau) + \kappa g_2(\sigma) - \lambda}{\lambda} \times 100\%. \quad (2)$$

If the error index assumes positive values, inequality (1) does not hold, it essentially means that the criterion predicts failure of the mechanical structure. On the other hand, if the error index assumes values less than or equal to zero the component is safe, according to the model.

5.2 Finite Element Fretting Fatigue Prediction

The numerical simulation was conducted aiming to determine the size of the finite element necessary to provide the correct fretting fatigue strength prediction within each data series considered. Two set of structured meshes ($l_c = 2.4\text{mm}$) each having l_e equal to 83 and $104\mu\text{m}$ were adopted to model the experimental data. For each set four different meshes were generated considering h_e values varying from 160 to $400\mu\text{m}$ as reported in Table 2. In this table the predicted critical contact size range a_{crit} is also reported for each value of h_e (these results concern the structured mesh where $l_e = 83\mu\text{m}$). The smallest value of this range corresponds to the greatest contact semi-width that presented non-positive values of I in the numerical simulation of the configuration tested, while the other value of the range is the smallest a where positive I values were computed. Notice that the error index is computed at every node of the mesh. The predicted range was obtained considering the node where I was maximum. Bolded data in Tab. 2 correspond to the predicted range which matched the experimental critical contact size range for a specific value of h_e for experimental series 1.

An alternative manner to present such results is depicted in Fig. 5. These graphs plot the fatigue criteria error index against the contact semi-width for $l_e = 83\mu\text{m}$. The two dashed vertical lines are used to define the experimental critical contact size range. It can be seen that for series 1 data the h_e value which predicts the correct contact size range is $h_e = 267\mu\text{m}$ for the Crossland and Mamiya&Araújo criteria and $h_e = 400\mu\text{m}$ for the Dang Van model.

Table 2. Critical contact sizes on series 1 with $l_c = 2.40\text{mm}$ and $l_e = 83\mu\text{m}$.

h_c (μm)	Critical contact size a_{crit} (mm)		
	Crossland	Dang Van	Mamiya&Araújo
160	0.10-0.19	0.10-0.19	0.10-0.19
200	0.19-0.28	0.10-0.19	0.19-0.28
267	0.28-0.38	0.19-0.28	0.28-0.38
400	0.38-0.57	0.28-0.38	0.38-0.57

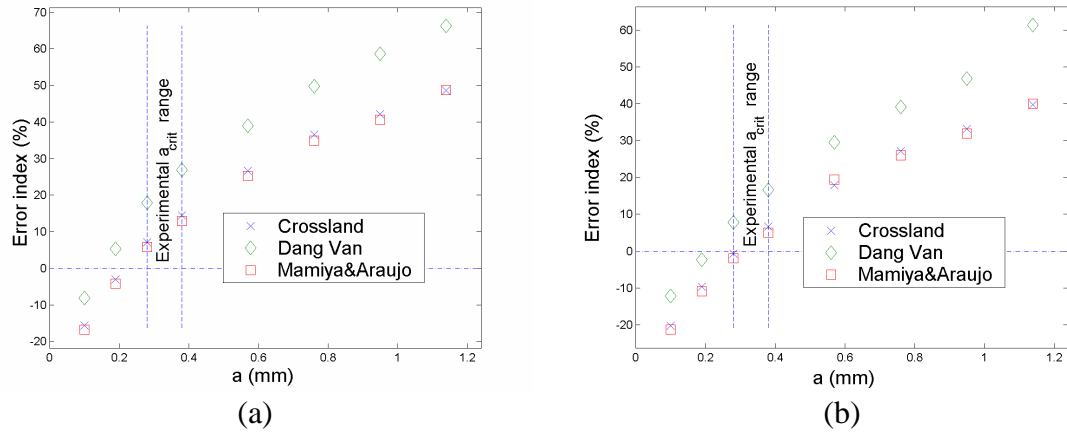


Figure 5. Error index for data series 1 with mesh parameters $l_e = 83\mu\text{m}$ and (a) $h_e = 200\mu\text{m}$ and (b) $h_e = 267\mu\text{m}$.

Tables 3 and 4 report the values of h_e necessary to predict the correct contact size range according to the multiaxial fatigue criteria considered in this work for $l_e = 83\mu\text{m}$ and $l_e = 104\mu\text{m}$, respectively. All values obtained are between 160 and 400 μm . To illustrate some of the results reported in Tab. 3 Figure 6 is used. It contains graphs of the Mamiya&Araújo error index versus element depth (h_e) for the critical contact size ranges of series 1 (fig. 6a) and 3 (fig. 6b) data. It can be observed in Fig 6a that the Mamiya&Araújo model predicts that the correct a_{crit} for series 1 data can be obtained for $h_e = 267\mu\text{m}$ while for series 3 values of h_e between 160 and 200 μm are required. Other graphs for different mesh characteristics and considering the other models assessed are not shown due to space limitation.

Table 3. Values of h_e that provide same fatigue strength results compared to experimental data using $l_e = 83\mu\text{m}$.

Series	h_e (μm)		
	Crossland	Dang Van	Mamiya&Araújo
1	267	400	267
2	267	400	267
3	160-200	267	160-200
4	200-267	267	200-267
5	160	200	160

Table 4. Values of h_e that provide same fatigue strength results compared to experimental data using $l_e = 104\mu\text{m}$.

Series	h_e (μm)		
	Crossland	Dang Van	Mamiya&Araújo
1	267	400	267
2	200-267	267	200
3	160-200	200-267	160
4	200-267	267	200
5	<160	200	<160

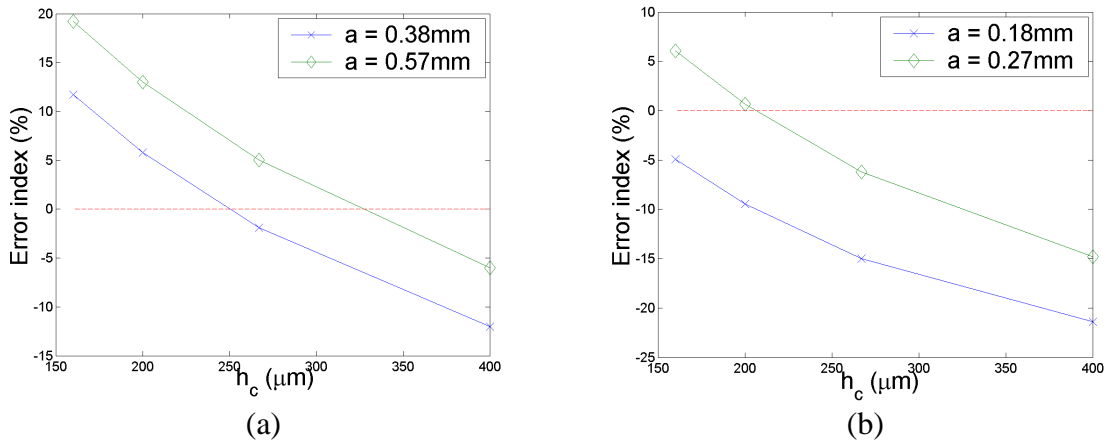


Figure 6. Error index for the critical contact size range values versus h_e using $l_e = 83\mu\text{m}$ and Mamiya&Araújo for data series (a) 1 and (b) 3.

6. DISCUSSION AND CONCLUSIONS

The analysis carried out in this work showed an alternative procedure to numerically compute the effect of the stress gradient in the prediction of fretting fatigue strength. It was shown that the choice of an appropriate mesh refinement level and element size is capable to successfully predict the critical contact size effect observed in Nowell's fretting experiments.

More specifically, it was found that the Crossland and the Mamiya&Araújo criteria required the same element size to predict the correct a_{crit} (table3), while Dang Van model presented a larger error index for the same element dimension.

Comparing the results of Tab. 3 ($l_e = 83\mu\text{m}$) with Tab. 4 ($l_e = 104\mu\text{m}$) it can be observed that the influence of the element width in the calculation for these l_e values was small, since slightly different values of h_e were reached in both cases.

In both set of structured meshes neither of the criteria studied found a unique range of element size (h_e range) capable to predict a_{crit} for all data considered. However, one should remember that: (i) the fatigue limit in torsion was estimated and this introduce inaccuracies to the analysis; (ii) the size of the element is determined based on the prediction provided by the multiaxial fatigue criteria, hence if such criteria are not working well for the tests considered they will provide a poor analysis. Notice that these models do not take in account the effect of the relative slip between the contacting surfaces on fretting life. Although this influence may not be very strong, since in the partial slip regime the amount of wear is small, it will certainly introduce some level of inaccuracy into the calculation.

It is worthy of notice that recent approaches (Naboulsi, 2003; Swalla, 2003) used to carry out a FE fretting fatigue strength analysis rely on the utilization of very fine meshes, which usually contain elements whose size is considerably smaller than a characteristic material grain size. For instance, the Al4%Cu alloy grain size is around $100\mu\text{m}$ (Nowell, 1988). It was observed that, in order to compute a stress field which closely agrees with the analytical solution for series 1 data and pad radius $R = 12.5$ mm an element with $h_e = 1.46\mu\text{m}$ and $l_e = 7.24\mu\text{m}$ was required. Besides being computationally very expensive such an approach seems to violate the continuum assumption.

7. REFERENCES

Araújo, J.A., 1998, On the initiation and arrest of fretting cracks, Doctor of Philosophy thesis, Oxford University.

Araújo, J.A., Nowell, D., 1999, Analysis of pad effects in fretting fatigue using short crack arrest methodologies, International Journal of Fatigue, 21, pp. 947-956.

Araújo, J.A. & Nowell, 2002, D., The effect of rapidly varying contact stress fields on fretting fatigue, International Journal of Fatigue, 24, pp. 763-775.

Bernardo, A.T.S., 2003, Fadiga por fretting: modelagem e simulação numérica, Projeto final de graduação, Universidade de Brasília.

Bernardo, A.T.S., Araújo, J.A., Mamiya, E.N., 2003, Determinação das distribuições de tensões em regiões de fretting via elementos finitos, Proc. of the 24th Iberian Latin-American Congress in Computational Methods in Engineering.

Bernardo, A.T.S., 2004, Fadiga por fretting: modelagem e simulação numérica, Master thesis, Universidade de Brasília.

Bramhall, R., 1973, Studies in fretting fatigue. Doctor of Philosophy thesis, Oxford University.

Castro, R.V., 2003, Metodologia para determinação do limiar da iniciação de trincas sob condições de fretting, Master thesis, Universidade de Brasília.

Crossland, B., 1956, Effect of large hydrostatic pressures on the torsional fatigue strength of an alloy steel, Proc. of the International Conference on Fatigue of Metal, IMechE.

Dang Van, K., Papadopoulos, I.V., 1987, Multiaxial fatigue failure criterion: a new approach, Proc. of the Third International Conference on Fatigue and Fatigue Thresholds.

Dantas, A.P., 2002, Incorporação de critérios de fadiga multiaxial em um programa de elementos finites, Master thesis, Universidade de Brasília, 2002.

Ferro, J.C.T., 2003, Fadiga com alto número de ciclos em entalhe, Projeto final de graduação, Universidade de Brasília.

Forrest, P.G., Fatigue of Metals, Pergamon Press: Oxford, pp.110-110, 1962.

Foutry, S., Elleuch, K. & Simeon, G., 2002, Prediction of crack nucleation under partial slip fretting predictions, Journal of Strain Analysis, 37, pp. 549-564.

Harish, G. & Farris, T. N., 1998, Effect of fretting contact stresses on crack nucleation in riveted lap joints, Proc. of the 39th AIAA/ASME/ASCE Structures, Structural Dynamics and Materials Conference, pp. 1-9.

Hills, D.A. & Nowell, D., 1994, Mechanics of Fretting Fatigue, Kluwe Academic Publishers: Dordrecht.

Kinyon, S.E., Hoeppner, D.W. & Mutoh, Y., (eds), 2002, Fretting fatigue: experimental and analytical results, ASTM STP 1425.

Mamiya, E.N., Araújo, J.A., 2002, Fatigue limit under multiaxial loadings: on the definition of the equivalent shear stress, Mechanics Research Communications, 29, pp.141-151.

Naboulsi, S. & Mall, S., 2003, Fretting fatigue crack initiation behaviour using process volume approach and finite element analysis, Triboloby International, 36, pp. 121-131.

Namjoshi, S.A., Mall, S., Jain, V.K. & Jin, O., 2002, Effects of process variables on fretting fatigue crack initiation in Ti-6Al-4V, Journal of Strain Analysis, 37, pp. 535-547.

Nowell, D., 1988, An analysis of fretting fatigue, Doctor of Philosophy thesis, Oxford University.

Papadopoulos, I.V., Davoli, P., Gorla, C., Filippini, M. & Bernasconi, A., 1997, A comparative study of multiaxial high-cycle fatigue for metals, *International Journal of Fatigue*, 29, pp. 219-235.

Ribó, R., Pasenau, M.A.R. & Escolano, E., 2000, GiD Reference Manual, International Center for Numerical Methods in Engineering (CIMNE), <http://gid.cimne.upc.es>.

Shaffer, S.J. & Glaeser, W.A., 1994, Fretting fatigue, *ASM fatigue and fracture handbook*.

Swalla, D.R. & Neu, R.W., 2003, Characterization of fretting fatigue process volume using finite element analysis, *Fretting Fatigue: Advances in Basic Understanding and Applications*, STP 1425, ASTM International.

Wittkowsky, B.U., Birch, P.R., 1999, Dominguez, J. & Suresh, S., An apparatus for quantitative fretting fatigue testing, *Fatigue Fract. Engng. Mater. Struct.*, 22, pp. 307-320.